Original Article

Toxicol. Res. Vol. 35, No. 2, pp. 167-179 (2019)
https://doi.org/10.5487/TR.2019.35.2.167

Open Access

www.ToxicolRes.org
Toxicological Research

α-Mangostin and Apigenin Induced Cell Cycle Arrest and Programmed Cell Death in SKOV-3 Ovarian Cancer Cells

Teeranai Ittiudomrak[1], Songchan Puthong[2], Sittiruk Roytrakul[3] and Chanpen Chanchao[4]

[1]*Program in Biotechnology, Faculty of Science, Chulalongkorn University, Bangkok, Thailand*
[2]*Institute of Biotechnology and Genetic Engineering, Chulalongkorn University, Bangkok, Thailand*
[3]*National Center for Genetic Engineering and Biotechnology (BIOTEC), National Science and Technology Development Agency, Pathum Thani, Thailand*
[4]*Department of Biology, Faculty of Science, Chulalongkorn University, Bangkok, Thailand*

Abstract

Ovarian cancer is the fifth main cause of pre-senescent death in women. Although chemotherapy is generally an efficient treatment, its side effects and the occurrence of chemotherapeutic resistance have prompted the need for alternative treatments. In this study, α-mangostin and apigenin were evaluated as possible anticancer alternatives to the chemotherapeutic drug doxorubicin, used herein as a positive control. The ovarian adenocarcinoma cell line SKOV-3 (ATCC No. HTB77) was used as model ovarian cancer cells, whereas the skin fibroblast line CCD-986Sk (ATCC No. CRL-1947) and lung fibroblast line WI-38 (ATCC No. CCL-75) were used as model untransformed cells. Apigenin and doxorubicin inhibited the growth of SKOV-3 cells in a dose- and time-dependent manner. After 72 hr exposure, doxorubicin was mostly toxic to SKOV-3 cells, whereas apigenin was toxic to SKOV-3 cells but not CCD-986Sk and WI-38 cells. α-Mangostin was more toxic to SKOV-3 cells than to CCD-986Sk cells. A lower cell density, cell shrinkage, and more unattached (floating round) cells were observed in all treated SKOV-3 cells, but the greatest effects were observed with α-mangostin. With regard to programmed cell death, apigenin caused early apoptosis within 24 hr, whereas α-mangostin and doxorubicin caused late apoptosis and necrosis after 72 hr of exposure. Caspase-3 activity was significantly increased in α-mangostin-treated SKOV-3 cells after 12 hr of exposure, whereas only caspase-9 activity was significantly increased in apigenin-treated SKOV-3 cells at 24 hr. Both α-mangostin and apigenin arrested the cell cycle at the G_2/M phase, but after 24 and 48 hr, respectively. Significant upregulation of *BCL2* (apoptosis-associated gene) and *COX2* (inflammation-associated gene) transcripts was observed in apigenin- and α-mangostin-treated SKOV-3 cells, respectively. α-Mangostin and apigenin are therefore alternative options for SKOV-3 cell inhibition, with apigenin causing rapid early apoptosis related to the intrinsic apoptotic pathway, and α-mangostin likely being involved with inflammation.

Key words: α-Mangostin, Apigenin, Apoptosis, Caspase activity, Cell cycle arrest, Ovarian cancer

INTRODUCTION

Ovarian cancer is the fifth main cause of pre-senescent (unnatural) death in women (1) and the most common cause of gynecological cancer-associated deaths (2). Among cervical, ovarian, and uterine cancers, ovarian cancer has reportedly caused the highest rate of deaths (3). Ovarian cancer, like other solid tumors, is associated with the deterioration of the intracellular structure, change in cellular adhesion, cell migration, invasion, proliferation, and angio-

Correspondence to: Chanpen Chanchao, Department of Biology, Faculty of Science, Chulalongkorn University, 254 Phayathai Road, Bangkok 10330, Thailand
E-mail: chanpen.c@chula.ac.th

Abbreviations: BCL2, B-cell lymphoma 2; CASP, Caspase; COX2, Cyclooxygenase 2; CTNNB1, Catenin beta 1; CTSB, Cathepsin B; GADPH, Glyceraldehyde 3-phosphate dehydrogenase; IL, Interleukin; NFκB, Nuclear factor kappa B.

pISSN: 1976-8257 eISSN: 2234-2753

genesis (4). It is a major problem for public health globally owing to its undefined signs and symptoms, making it essentially asymptomatic until at an advanced stage and thus preventing its early diagnosis and treatment. For decades, surgery and chemotherapy, especially platinum- or taxol-based chemotherapy as well as the more recent monoclonal antibody-directed bevacizumab, have been introduced for ovarian cancer treatment, but these procedures are not fully effective because of their adverse side effects and the advent of chemoresistance (5). Hence, novel or alternative treatments are necessary for the treatment of patients with ovarian cancer.

Natural products, especially herbs, have gained increasing attention for use in ovarian cancer therapy to inhibit the proliferation and induce apoptosis of the cancer cells, with the potential benefits of less side effects and reduced resistance (for now) (6). Thus, many natural compounds or chemicals have been isolated, mainly from plants (e.g., cryptotanshinone in the traditional Chinese herbal medicine *Salvia miltiorrhiza* Bge. (7)), and the molecular mechanisms of action of some of these compounds have been reported. For example, proanthocyanidins from the leaves of Chinese bayberry (*Myrica rubra* Sieb. et Zucc.) showed strong inhibitory effects against cell growth (with cell cycle arrest at the G_1 phase), angiogenesis, and the migration and invasion of A2780/CP70 cisplatin-resistant ovarian cancer cells (8). In addition to natural compounds, synthetic compounds have been reported to be promising therapeutic sources. For example, synthesized (1*E*,4*E*)-6-(1-(isopentyloxy)nonyl)-5-methoxynaphthalene-1,4-dione dioxime, which is a derivative of 1,4-naphthoquinone oxime, was reported to be strongly toxic to the ovarian cancer cell line A2780, with a half maximal inhibitory concentration (IC_{50}) value of 8.26 ± 0.22 μM (9). Furthermore, O^2-(acetoxymethyl)-1-(*iso*-butylamino)diazen-1-ium-1,2-diolate and O^2-(acetoxymethyl)-1-(isopropylamino)diazen-1-ium-1,2-diolate, synthesized from primary amine-based diazeniumdiolates, reduced the proliferation of SKOV-3 and ES2 ovarian cancer cells at 0.033-1.0 mg/mL after 24 hr of exposure (10).

In this study, α-mangostin and apigenin were focused on as possible therapeutic agents because both can be isolated from many natural products in Thailand. α-Mangostin is mainly isolated from the pericarp of *Garcinia mangostana* (11) and the cerumen of the stingless bee *Tetragonula laeviceps* (12), whereas apigenin is the main compound extracted from Roman chamomile (*Chamaemelum nobile* (L.)) (13) and bee pollen (*Apis mellifera*) (14). Both compounds have been reported to have many bioactivities, including anti-biofilm formation (15), anti-aging (16), anti-inflammatory (17), and anti-gout (18) activities. Furthermore, only a few studies have been reported on the contribution of both compounds to SKOV-3 ovarian cancer prevention. Considering only gynecological cancers, α-mangostin has been reported to inhibit the growth of HeLa human cervical cancer cells (19), but there are no reports on its effect on the SKOV-3 ovarian cancer cell line. For apigenin, only a few studies on its effect on the SKOV3 cancer cell line are available (20,21). Thus, more data on these two natural compounds are necessary.

The aim of this present study was to evaluate the *in vitro* toxicity of α-mangostin and apigenin in SKOV-3 ovarian cancer cells in comparison with that in the untransformed CCD-986Sk skin fibroblast and WI-38 lung fibroblast lines as model normal human cells, using the 3-[4,5-dimethylthiazol-2-yl]-2,5-diphenyltetrazolium bromide (MTT) assay. Changes in the morphology of the treated cells were observed by light microscopy. Programmed cell death was investigated by flow cytometry following annexin V-Alexa Fluor 488 and propidium iodide (PI) staining, whereas cell cycle arrest was likewise investigated after PI staining only. The activities of caspase-3, -8, and -9 were also evaluated, and changes in the transcript expression levels of representative inflammation-associated genes, proto-oncogenes, autophagy-associated genes, and apoptosis-associated genes were investigated by the quantitative real-time reverse-transcription polymerase chain reaction (RT-qPCR). Overall, the data obtained provide a broader insight into how α-mangostin and apigenin inhibit the growth of SKOV-3 ovarian cancer cells.

MATERIALS AND METHODS

Cell culture. The human ovarian adenocarcinoma-derived cell line SKOV-3 (ATCC No. HTB77) was cultured in McCoy's 5A (modified) medium supplemented with 10% (v/v) fetal calf serum (FCS). The untransformed (normal) human skin fibroblast line CCD-986Sk (ATCC No. CRL-1947) and lung fibroblast line WI-38 (ATCC No. CCL-75) were used for direct comparison with SKOV-3. Both CCD-986Sk and WI-38 cells were cultured in Eagle's Minimum Essential Medium (MEM) supplemented with 10% (v/v) FCS. All three cell lines were cultured and tested at 37°C with 5% (v/v) CO_2 in a humidified environment.

MTT assay of cell viability and proliferation. CCD-986Sk and WI-38 cells were seeded at 1×10^4 cells/well in 96-well plates containing 200 μL of medium for overnight culture, whereas SKOV-3 cells were cultured in the same manner but seeded at 5×10^3 cells/well. Then, the cells were treated with various concentrations of apigenin, α-mangostin, or doxorubicin, or the 0.1% (v/v) dimethyl sulfoxide (DMSO) solvent only (control). The SKOV-3 cells were treated for 24, 48, and 72 hr, whereas the CCD-986Sk and WI-38 cells were treated for 24 hr only. After the indicated incubation (exposure) time was reached, 10 μL of 5 mg/mL MTT solution was added to each well and the culture plates were incubated for 3 hr to allow for-

mazan formation. The culture medium was then removed, the formazan was solubilized by the addition of 150 μL of DMSO, and the absorbance at 560 nm (A_{560}) was measured with a microplate reader. The cell viability (%) was calculated using Eq. (1) as follows:

$$\text{Cell viability (\%)} = 100 \times (A_{560}\text{ treated cells} - A_{560}\text{ blank})/(A_{560}\text{ untreated cells} - A_{560}\text{ blank}) \quad (1)$$

The IC_{50} value of each compound was calculated from the graphical plot of the relative number of viable cells (%) *vs*. the test compound concentration.

Cell imaging. Test cells at 5×10^5 cells in 5 mL of medium in a 25-cm^2 flask were cultured overnight and treated the next day with 0.1% (v/v) DMSO alone (control) or DMSO containing α-mangostin (7.309 μM), apigenin (18.502 μM), or doxorubicin (0.431 μM) for 24, 48, and 72 hr. Live cell images were captured using a Nikon Eclipse TS100 microscope coupled with a DS-L3 imaging system at 40×, 100×, and 200× magnifications.

Apoptosis and cell cycle analysis. The test cells were cultured as described in the Cell imaging section above and harvested at the indicated times by trypsinization with 0.05% (w/v) trypsin in 0.5 mM ethylenediaminetetraacetic acid buffer. The cells were then washed twice with cold phosphate-buffered saline (PBS), using centrifugation at 3,000 × *g* for 5 min at 4°C to harvest the cells each time. For apoptosis detection, the cell pellets were resuspended in 50 μL of binding buffer (10 mM HEPES, pH 7.4, 140 mM NaCl, and 2.5 mM $CaCl_2$) and stained with 5 μL of annexin V-Alexa Fluor 488 and 5 μL of PI for 30 min at room temperature in the dark. For the cell cycle study, the cell pellets were fixed in 200 μL of cold 70% (v/v) ethanol at –20°C overnight, harvested, and washed as described above. The washed cell pellet was then suspended in 250 μL of PBS containing 0.1 mg/mL RNase A and incubated at 37°C for 30 min. Thereafter, it was washed as described above, resuspended in staining buffer (12.5 μL of 1 mg/mL PI in PBS), and incubated at room temperature for 30 min in the dark. The samples were then analyzed by flow cytometry on a FC 500 MPL cytometer (Beckman Coulter, Brea, CA, USA) that recorded 10,000 events per sample. The experiment was performed in triplicate.

Caspase activity assay. The test cells were plated and treated as described above for the apoptosis and cell cycle studies. The treated cells were harvested by trypsinization at 12 and 24 hr and then tested with caspase-3, -8, and -9 colorimetric assay kits (Catalog No. ab39401, ab39700, and ab65608, respectively; Abcam, Cambridge, UK) according to the manufacturer's instructions. In brief, the harvested cells were washed with cold PBS and centrifuged at 800 × *g*. The cell pellet was then lysed by the addition of 50 μL of chilled cell lysis buffer and incubation on ice for 10 min. The lysed mixture was clarified by centrifugation at 10,000 × *g* for 1 min and the supernatant was transferred to a new microcentrifuge tube. The protein concentration in the supernatant of each sample was measured using the Bradford assay and then adjusted to 100 μg of protein per 50 μL of cell lysis buffer for subsequent application to each well of a 96-well plate. Next, 50 μL of 2× reaction buffer containing dithiothreitol at a final concentration of 10 mM was added into each sample well. After mixing, the respective substrate of each caspase was added to each well and the plate was incubated at 37°C for 1-2 hr. Finally, the absorbance of each reaction at 400-405 nm was measured on a microplate reader. Each experiment was performed in triplicate.

Analysis of transcript expression levels by RT-qPCR. The cell lines were treated and processed as described previously for the apoptosis detection assay until the cell pellet was collected. After cell harvesting, total RNA from each sample was extracted using an RNeasy mini kit (Catalog No. 74104; Qiagen, Valencia, CA, USA). The RNA concentration and purity were evaluated by spectrophotometry at an absorbance of 260 and 280 nm, respectively. The RT-qPCR was performed using the One-Step SYBR® PrimeScript™ RT-PCR Kit II (Perfect Real Time; Catalog No. R086A; Takara, Tokyo, Japan). The PCR mixture contained 20 ng of total RNA, 0.4 μM of both forward and reverse primers, 1 μL of PrimeScript™ Enzyme Mix II, and 1× One-Step SYBR® RT-PCR Buffer IV. The nucleotide sequences of the primers used in this study are listed in Table 1.

Amplification and quantification of each gene of interest were performed using the Minicon® system (Bio-Rad, Hercules, CA, USA). Thermocycling was performed as follows. First, the total RNA was reverse transcribed into cDNA at 42°C for 5 min. Then, qPCR was performed with an initial 95°C for 10 s, followed by 40 cycles of 95°C for 10 s and 60°C for 30 s. Dissociation analysis was performed to validate the specific product for each primer pair. The expression level of all target genes was normalized to that of *GADPH* in each sample and compared as the relative expression level between the control and treated samples.

Statistical analysis. Data are presented as the mean ± one standard deviation (1SD), derived from three independent repeats in each experiment. The data were analyzed by one-way analysis of variance (ANOVA) followed by Tukey's multiple-comparisons test for the significance of differences between the means. Significance was accepted at the $p < 0.01$ and $p < 0.05$ levels. All analyses were performed using the SPSS version 19.0 program (IBM corporation, Chicago, IL, USA).

Table 1. Targeted genes and primers used for their amplification by RT-qPCR

Gene	Forward primer (5′→3′)	Reverse primer (5′→3′)
Reference gene		
GADPH	GGGCATCCTGGGCTACTCTG	GAGGTCCACCACCCTGTTGC
Inflammation-associated genes		
COX2	TCTGCAGAGTTGGAAGCACTCTA	GCCGAGGCTTTTCTACCAGAA
NFκB	ATGGCTTCTATGAGGCTGAG	GTTGTTGTTGGTCTGGATGC
Proto-oncogene		
CTNNB1	CTTGTGCGTACTGTCCTTCG	AGTGGGATGGTGGGTGTAAG
Autophagy-associated gene		
CTSB	CAGCGTCTCCAATAGCGA	AGCCCAGGATGCGGAT
Apoptosis-associated genes		
BCL2	ATGTGTGTGGAGACCGTCAA	GCCGTACAGTTCCACAAAGG
CASP3	TGTTTGTGTGCTTCTGAGCC	CACGCCATGTCATCATCAAC
CASP7	CCAATAAAGGATTTGACAGCC	GCATCTGTGTCATTGATGGG
CASP8	GATCAAGCCCCACGATGAC	CCTGTCCATCAGTGCCATAG
CASP9	CATTTCATGGTGGAGGTGAAG	GGGAACTGCAGGTGGCTG

GADPH, glyceraldehyde 3-phosphate dehydrogenase; *COX2*, cyclooxygenase 2; *NFκB*, nuclear factor kappa B; *CTNNB1*, catenin beta 1; *CTSB*, cathepsin B; *BCL2*, B-cell lymphoma 2; *CASP*, caspase.

Table 2. IC_{50} values of α-mangostin, apigenin, and doxorubicin for SKOV-3 cells

Compound	IC_{50} value (μM) at an incubation time of:		
	24 hr	48 hr	72 hr
α-Mangostin	2.466 ± 0.338	2.977 ± 0.054	3.062 ± 0.349
Apigenin	26.538 ± 6.024	21.175 ± 5.249**	18.197 ± 3.095**
Doxorubicin	0.534 ± 0.084	0.343 ± 0.023	0.117 ± 0.008

**Indicates a significant difference to the IC_{50} value of 24 hr when treated with the same compound.

RESULTS

In order to determine the cytotoxic IC_{50} values of α-mangostin, apigenin, and doxorubicin for direct comparison (Table 2, 3, Fig. 1, 2), SKOV-3 ovarian cancer cells were cultured on a small scale (5×10^3 cells in 200 μL of medium in each well of a 96-well plate). With regard to the viability of the treated SKOV-3 cells, α-mangostin, apigenin, and doxorubicin all clearly inhibited cell growth in a dose-dependent manner (Fig. 1). Both apigenin and doxorubicin also showed a time-dependent inhibition, but not α-mangostin. However, at any given time point, α-mangostin was more toxic to the SKOV-3 cells than apigenin was, with the cytotoxicity being 10.8-fold at 24 hr to 5.9-fold higher at 24 and 72 hr, respectively (Table 2). All three compounds affected the number of viable cells and growth of SKOV-3 cells from an early exposure time (24 hr). The longer the exposure to apigenin, the significantly lower was the IC_{50} value, but the compound still remained less inhibitory than α-mangostin and, especially, doxorubicin.

Table 3. IC_{50} values of α-mangostin, apigenin, and doxorubicin for CCD-968Sk and WI-38 cells after 24 hr of treatment

Compound	IC_{50} value (μM)	
	CCD-986Sk cells	WI-38 cells
α-Mangostin	9.805 ± 3.169	1.502 ± 0.464
Apigenin	ND	36.873 ± 0.971
Doxorubicin	ND	0.604 ± 0.156

ND = not determined.

After 24 hr of exposure, apigenin was nontoxic to CCD-986Sk and WI-38 cells, in contrast to α-mangostin. The IC_{50} value of apigenin for CCD-986Sk cells was not obtained since it resulted in 70% cell survival even at a high concentration of the compound (92.510 μM) (Fig. 2, Table 3); furthermore, the relative cell survival of 100% detected at 1.156-55.506 μM indicated that apigenin did not affect cell proliferation/survival (Fig. 2B). Likewise for WI-38 cells, apigenin at 1.156-2.313 μM did not affect the cell growth, and a concentration of up to 27.753 μM was nontoxic to the cells (Fig. 2B). Although α-mangostin was toxic to CCD-986Sk cells, the cytotoxicity was about 4-fold less than that in SKOV-3 cells. As with apigenin, the IC_{50} value of doxorubicin for CCD-986Sk cells was not obtained since the compound did not affect the

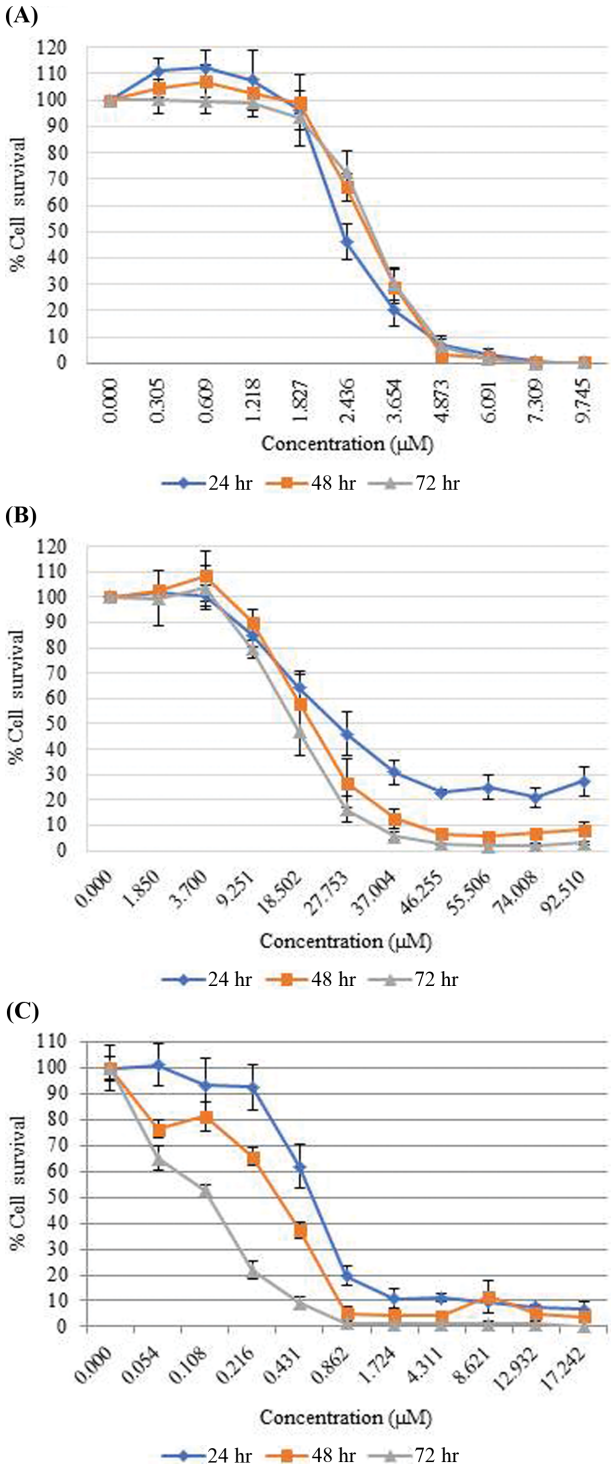

Fig. 1. Toxicity of (A) α-mangostin, (B) apigenin, and (C) doxorubicin in SKOV-3 cells. Cell survival (%) was estimated after treatment for 24, 48, and 72 hr (blue, orange, and grey lines, respectively). Data are shown as the mean ± 1SD, derived from three independent repeats.

growth of this cell line. However, for WI-38 cells, doxorubicin was more cytotoxic than α-mangostin (Table 3).

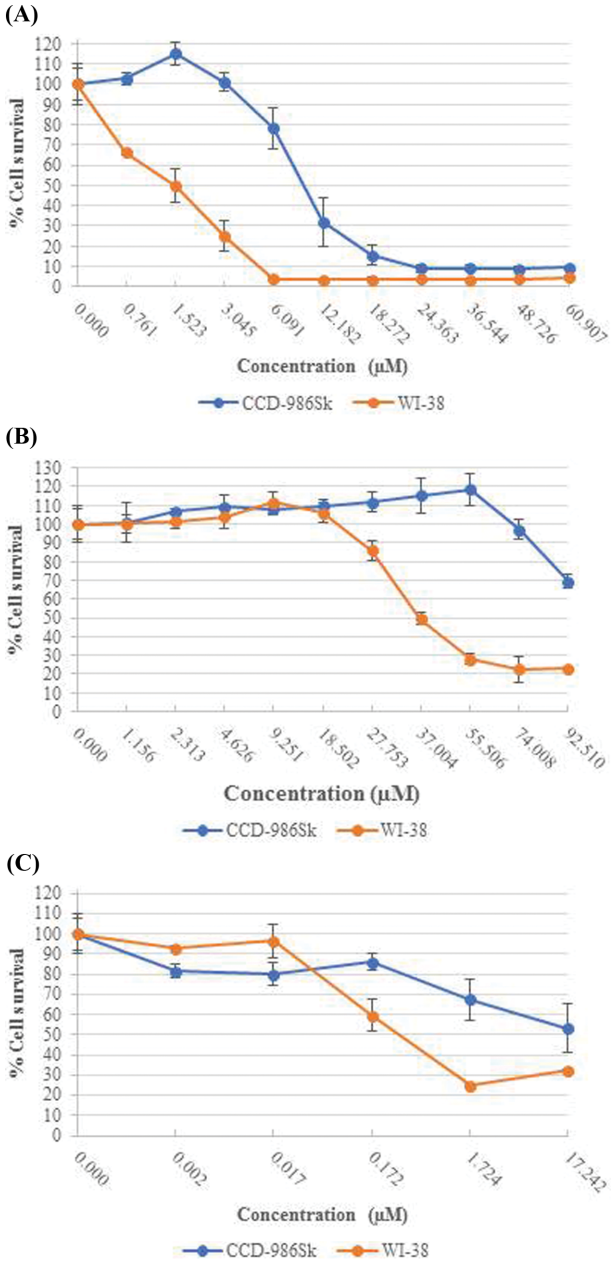

Fig. 2. Toxicity of (A) α-mangostin, (B) apigenin, and (C) doxorubicin in CCD-986Sk skin fibroblasts (blue line) and WI-38 lung fibroblasts (orange line). Cell survival (%) was estimated after 24 hr of treatment. Data are shown as the mean ± 1SD, derived from three independent repeats.

For all the other experiments, the SKOV-3 cells were cultured on a larger scale at 5×10^5 cells in 5 mL of medium in T25 flasks. Since α-mangostin treatment of the SKOV-3 cells at the IC_{50} value obtained from the small-scale (200 μL) culture (Table 2) was not effective at all in the larger-scale cultures, the concentration of α-mangostin was increased to 3× the IC_{50} value. The most obvious changes observed are summarized in Fig. 3-7. Hence, the

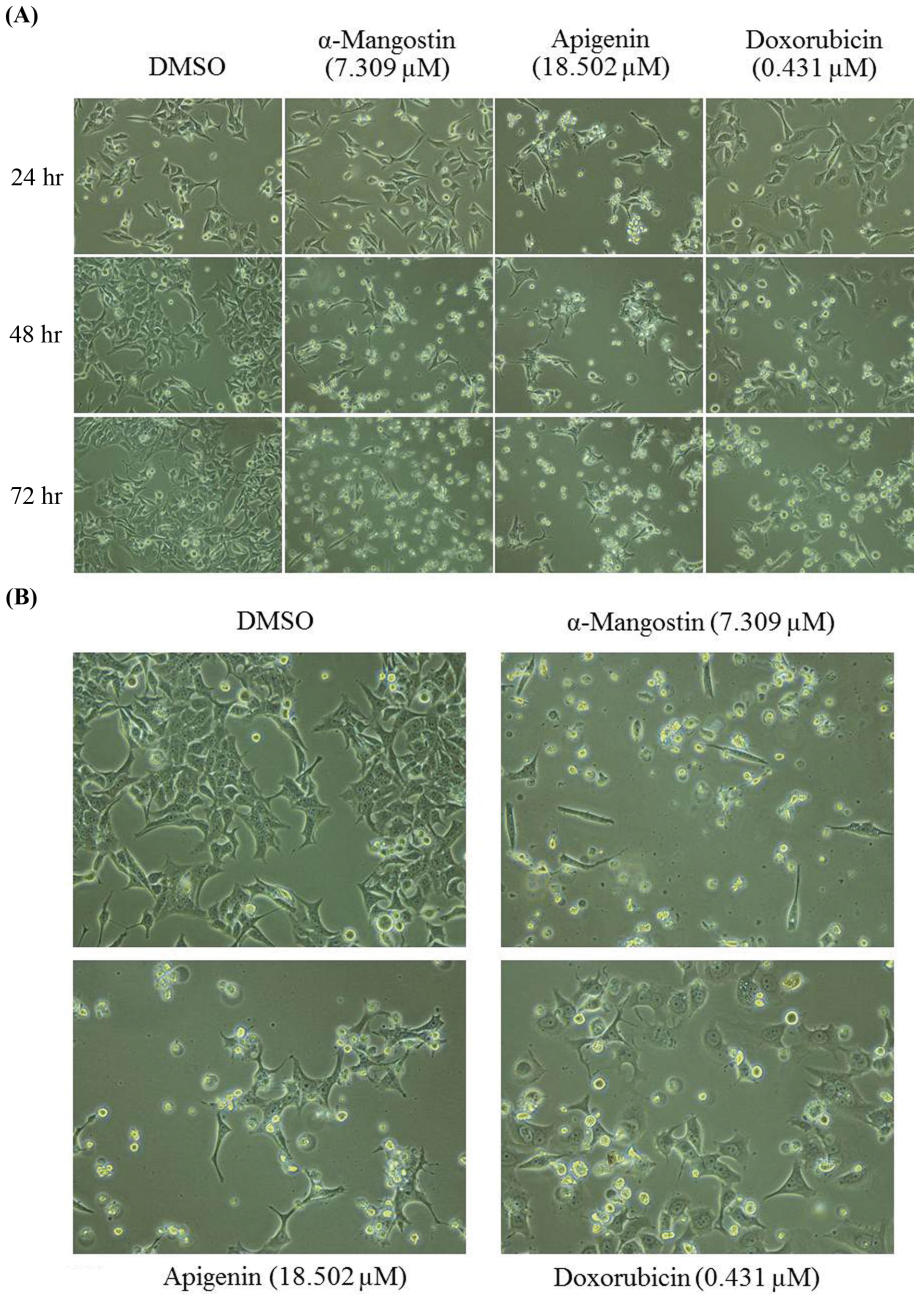

Fig. 3. Morphology of SKOV-3 cells treated with 0.1% (v/v) dimethyl sulfoxide (DMSO) alone or DMSO containing α-mangostin (7.309 μM), apigenin (18.502 μM), or doxorubicin (0.431 μM) for (A) 24, 48, and 72 hr (100× magnification) and (B) after 48 hr (200× magnification). Images shown are representative of those seen from at least three such fields of view per sample and three independent repeats.

potency of α-mangostin at any given concentration depended directly on the density and amount of cells as well as its dose. This phenomenon has been reported before (22-24). Morphological changes in the treated SKOV-3 cells were evident at the later exposure times compared with the control (DMSO-treated cells). After 24 hr of exposure, the SKOV-3 cells treated with each test compound looked somewhat similar to the control cells; however, after 48 and 72 hr, the treated cells had a lower cell density and a higher proportion of unadhered and round cells (Fig. 3A). At the higher magnification of 200×, it was evident that after 48 hr of exposure, the α-mangostin-treated SKOV-3 cells were mostly damaged, with very few spindle-shaped cells present. Cell shrinkage was observed in the α-mangostin- and apigenin-treated SKOV-3 cells, whereas some cell blebbing was seen in the doxorubicin-treated cells. In

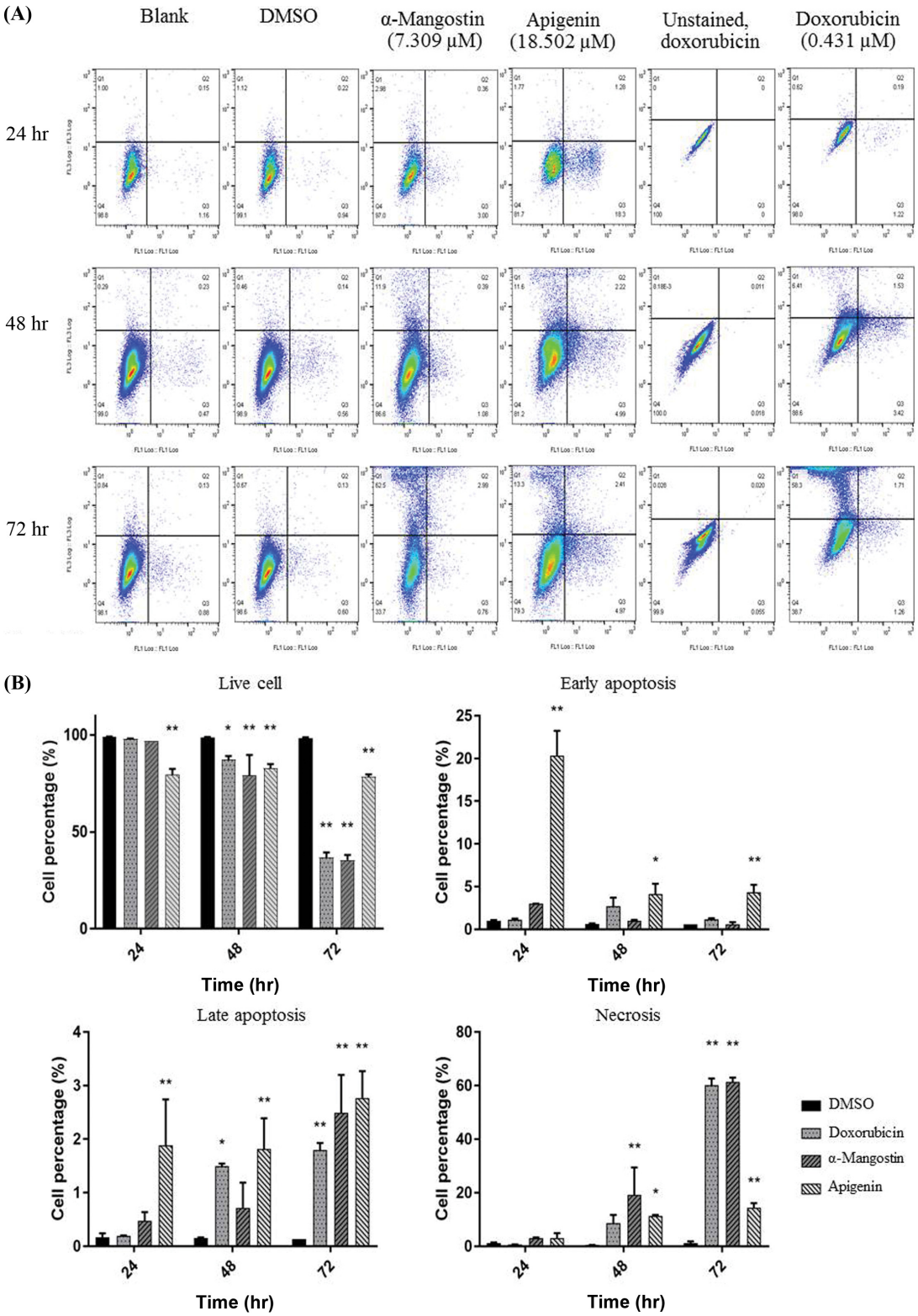

Fig. 4. Flow cytometric analysis of SKOV-3 cells stained for annexin-V and propidium iodide (PI) after incubation of cells in 0.1% (v/v) dimethyl sulfoxide (DMSO) alone or DMSO containing α-mangostin (7.309 μM), apigenin (18.502 μM), or doxorubicin (0.431 μM) for 24, 48, and 72 hr. (A) FACS profiles and (B) derived histogram analyses are shown for 10,000 events and are representative of those seen from three replications. * and ** represent a significant difference between the control and treated cells at $p < 0.05$ and $p < 0.01$, respectively.

addition, the apigenin- and doxorubicin-treated SKOV-3 cells had more vacuoles (Fig. 3B).

Since a lower density of cells was observed after a longer exposure to α-mangostin, apigenin, and doxorubicin, suggesting cell death as well as inhibition of proliferation, the possibility of the induction of programmed cell death was further investigated. The SKOV-3 cells were treated with the same concentration of each reagent as used for evaluating the change in morphology. Programmed cell death can be analyzed by staining target cells with annexin V and PI, whereas cell cycle arrest can be investigated by staining target cells with PI alone. In both cases, the staining level for each cell can be quantitatively determined using flow cytometry.

Since apoptosis causes a loss of membrane phospholipid asymmetry (25), the phosphatidylserine that is normally located in the cytosol is flipped outside, allowing annexin V (conjugated with Alexa fluor 488) to bind to it. Thus, the annexin V-Alexa fluor 488 conjugate can bind to apoptotic but not to viable cells. At a longer time beyond death, necrotic cells have an even more damaged and leaky membrane that allows PI to pass into the nucleus and bind to the DNA. Thus, viable cells are negative for both annexin V-Alexa fluor 488 and PI staining, showing only autofluorescence. Apoptotic cells will be positive for annexin V-Alexa fluor 488 (green fluorescence) but negative for PI staining, whereas necrotic cells will be positive for both annexin V-Alexa fluor 488 and PI staining (red and green fluorescence, respectively) (26). Flow cytometry can also be used to quantitatively analyze cell cycle arrest, where the amount of bound PI (and thus red fluorescence) equates to the amount of DNA; thus, the cell cycle position (subphases G_1, S, and G_2/M) is identified by the DNA content through PI staining.

After staining with annexin V-Alexa fluor 488 and PI, it was evident that apigenin had caused a significant level of early and late apoptosis from 24 hr onwards, but with less early apoptosis at the later time points, and subsequently caused significant necrosis, especially at 72 hr (Fig. 4). On the other hand, doxorubicin caused a significant level of both late apoptosis and necrosis, but only after a longer exposure of 72 hr. Although α-mangostin gave a similar result to doxorubicin, the level of necrosis was significantly increased and detected slightly earlier (from 48 hr) than the 72 hr time span for the other compounds (Fig. 4).

From Fig. 4, it was evident that the programmed cell death of the SKOV-3 cells was induced by each of the three compounds and that it involved apoptosis (early and/or late). Hence, apoptosis was further investigated by evaluating the cellular caspase activity. As is known, both

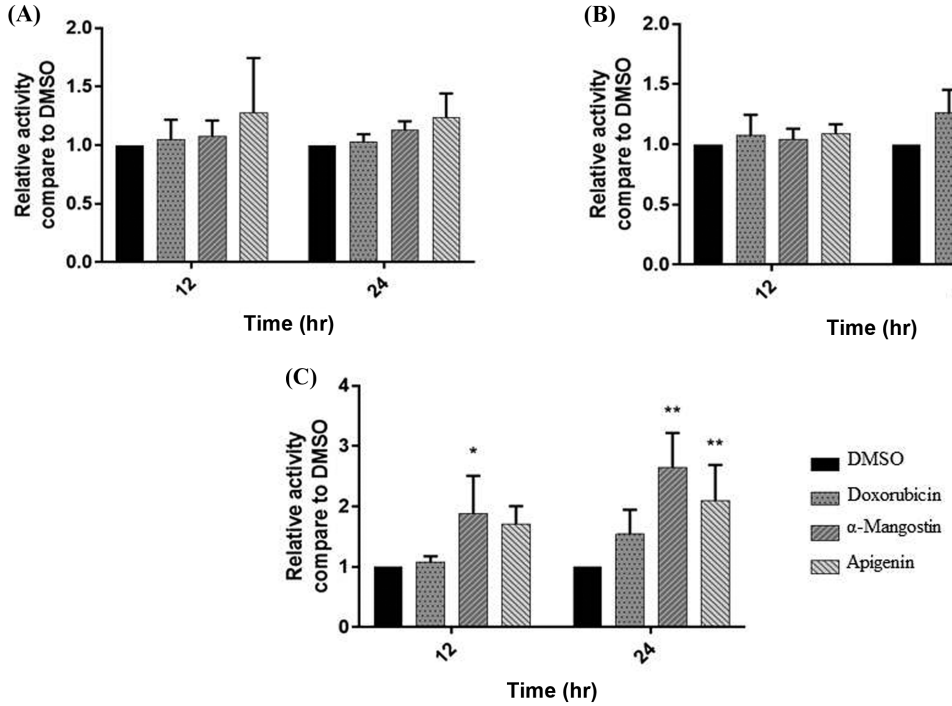

Fig. 5. Relative caspase activity in doxorubicin-, α-mangostin-, and apigenin-treated SKOV-3 cells. Cells were treated with 0.1% (v/v) dimethyl sulfoxide (DMSO) alone (control) or DMSO containing α-mangostin (7.309 μM), apigenin (18.502 μM), or doxorubicin (0.431 μM) for 12 and 24 hr and then assayed for (A) caspase-8, (B) caspase-9, and (C) caspase-3 activity. Data are shown as the mean ± 1SD, derived from three replications, where * and ** represent a significant difference between the control and treated cells at $p < 0.05$ and $p < 0.01$, respectively.

caspase-8 and caspase-9 are involved in the intrinsic pathway, whereas the apoptosis-mediating caspase-3 is involved in both the extrinsic and intrinsic pathways. Herein, the very early exposure time (12 and 24 hr) to each compound was evaluated. The activity of caspase-3 was significantly ($p < 0.05$) increased in the α-mangostin-treated SKOV-3 cells after 12 hr of exposure, while its activity was also significantly ($p < 0.01$) increased in both the α-

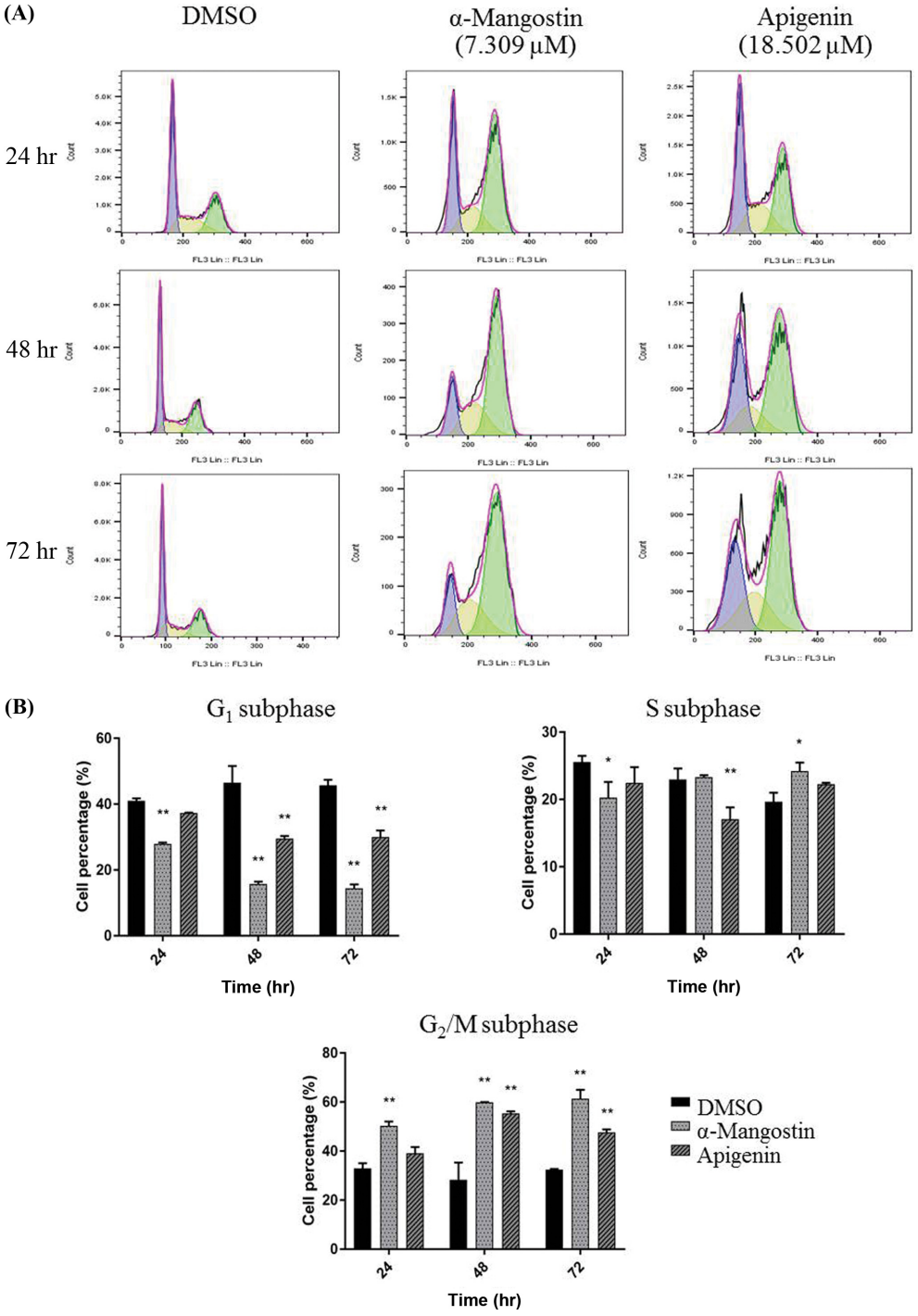

Fig. 6. Cell cycle arrest of SKOV-3 cells after treatment with 0.1% (v/v) dimethyl sulfoxide (DMSO) alone (control) or DMSO containing α-mangostin (7.309 μM) or apigenin (18.502 μM) for 24, 48, and 72 hr. (A) Flow cytometric histograms (5,000 events) representative of those seen from three replications, and (B) the derived mean % (± 1SD) of cells in each phase of the cell cycle after 24, 48, and 72 hr treatment. * and ** represent a significant difference between the control and treated cells at $p < 0.05$ and $p < 0.01$, respectively.

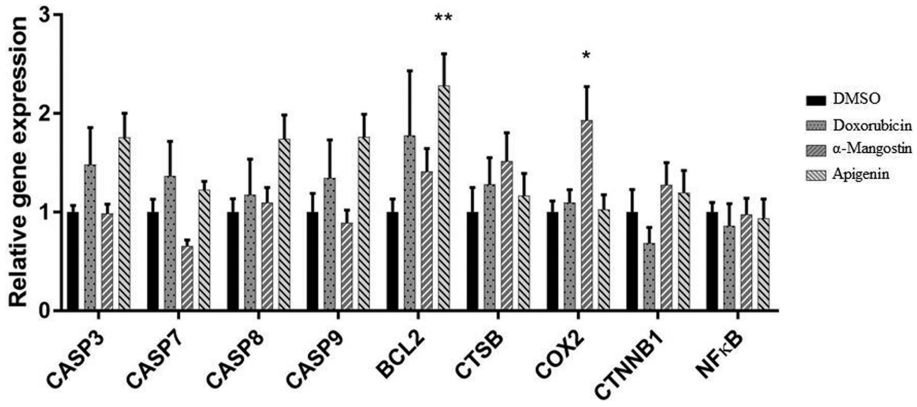

Fig. 7. Changes in the transcript expression levels of the selected inflammation-associated genes (*COX2* and *NFκB*), proto-oncogene (*CTNNB1*), autophagy-associated gene (*CTSB*), and apoptosis-associated genes (*BCL2*, *CASP3*, *CASP7*, *CASP8*, and *CASP9*). SKOV-3 cells were cultured with 0.1% (v/v) dimethyl sulfoxide (DMSO) alone (control) or DMSO containing α-mangostin (7.309 μM), apigenin (18.502 μM), or doxorubicin (0.431 μM) for 24 hr. Data are shown as the mean ± 1SD, derived from three independent repeats. * and ** represent a significant difference between the control and treated cells in each group at $p < 0.05$ or $p < 0.01$, respectively.

mangostin- and apigenin-treated cells after 24 hr of exposure, but the numerical increase observed in the doxorubicin-treated cells was not significant (Fig. 5). Caspase-8 activity was not significantly changed by all three treatments at both time points. Although the caspase-9 level was numerically increased in all treatments at 24 hr, it was only statistically significant ($p < 0.01$) for the apigenin-treated SKOV-3 cells. Thus, it may be possible that the early apoptosis induced by apigenin in SKOV-3 cells at 24 hr was influenced by the intrinsic pathway.

Next, we evaluated if cell cycle arrest was induced in the SKOV-3 cells by these compounds. After 24 hr of exposure, α-mangostin had induced arrest at the G_2/M phase ($p < 0.01$), whereas apigenin likewise arrested the cells only after 48 hr of exposure (Fig. 6). Thus, α-mangostin caused cell cycle arrest faster than apigenin, which concurs with α-mangostin being more toxic to the SKOV-3 cells (Table 2).

To determine in deeper detail how α-mangostin and apigenin affect the proliferation or death of SKOV-3 cells, changes in the transcript expression levels of selected genes from four groups were investigated. The first group was inflammation-associated genes, of which cyclooxygenase 2 (*COX2*) and nuclear factor kappa B (*NFκB*) were representatives. The second group was proto-oncogenes, from which catenin beta 1 (*CTNNB1*) was selected. The third group was autophagy-associated genes, with cathepsin B (*CTSB*) being a representative. The last group was apoptosis-associated genes, from which B-cell lymphoma 2 (*BCL2*), and the caspase genes *CASP3*, *CASP7*, *CASP8*, and *CASP9* were selected. The data are summarized in Fig. 7. Although a trend of mostly an increase in the gene expression level relative to that in the control cells was numerically observed for all tested genes (except for *NFκB*) among the different treatments, the upregulation was significant only for *BCL2* ($p < 0.01$) and *COX2* ($p < 0.05$) in the apigenin- and α-mangostin-treated SKOV-3 cells, respectively.

DISCUSSION

α-Mangostin extracted from the cerumen of *Tetragonula laeviceps* was reported to have potent cytotoxicity against several types of cancer cell lines, including the breast cancer BT474, undifferentiated lung cancer Chago, hepatoblastoma Hep-G_2, gastric carcinoma KATO-III, and colon adenocarcinoma SW620 cell lines, with IC_{50} values that ranged from 0.88 ± 0.16 to 2.25 ± 0.20 μM (12). Some of the molecular details on how α-mangostin inhibits the growth of BT474 cells have been under continuous study in our laboratory. With some congruence, breast and gynecological cancers, especially ovarian cancer, have been reported to be related to each other owing to their similar genetic basis (27), while a patient with breast cancer was later found to have primary ovarian small cell carcinoma and endometrioid adenocarcinoma of the uterus (28). Indeed, an increased risk of breast and ovarian cancers has been reported to be associated with germline mutations in *BRCA1* and *BRCA2* (29). This led us to investigate the role of α-mangostin in SKOV-3 ovarian cancer cells.

There have been diverse reports that oxidative stress, chronic inflammation, and cancer are closely linked (30-32). Not only do reactive oxygen species (which cause oxidative stress in cells) damage biological molecules, but they can also lead to chronic inflammation and eventually mediate chronic diseases such as cancer (30). In addition, the oxidative stress caused by the abnormal activation of nuclear factor E2-related factor 2 due to epigenetic alterations can increase anticancer drug resistance (33). Thus, finding an antioxidant or a free-radical-scavenging compound is likely to be beneficial for preventing cancer. Api-

genin is a major compound extracted from *Apis mellifera* bee pollen and was reported to have free-radical-scavenging activity (14). Thus, in this work, we evaluated if it could inhibit the growth of SKOV-3 ovarian cancer cells.

Different naturally occurring compounds can inhibit the growth of SKOV-3 cells to different extents and potentially by different mechanisms. In this work, apigenin was clearly toxic to SKOV-3 cells but not to normal cells. α-Mangostin showed an almost similar toxicity as that of doxorubicin to SKOV-3 cells, but it was unfortunately also toxic to the WI-38 normal lung fibroblasts. α-Mangostin at less than 6.091 μM was safe for CCD-986Sk skin fibroblasts (Table 3). Thus, the cell-type specificity is of concern and has been reported before (34-37). Although α-mangostin was more toxic than doxorubicin to the normal CCD-986Sk skin fibroblasts, it was less toxic than doxorubicin to the normal WI-38 lung fibroblasts. Aside from the data obtained indicating that finding an alternative compound for the antiproliferation of SKOV-3 cancer cells is still needed, the application of α-mangostin in broad systemic application for cancer prevention and treatment must be of some concern. It has been suggested that the plant-based metallic nanoparticles synthesized from *Abutilon inducum*, *Butea monosperma*, *Gossypium hirsutum*, *Indoneesiella echioides*, and *Melia azedarach* were toxic to cancer cells and not to normal cells (38).

Because both α-mangostin and apigenin induced apoptosis, but after different exposure times, the activities of caspase-3, -8, and -9 were assayed. Although late apoptosis and necrosis were clearly detected after 72 hr, the significant increase in activity of caspase-3 (the final executor of apoptosis and the most significant member of the apoptotic pathway) was investigated after a 12-hr exposure in order to optimize the detection of this early apoptotic response. After exposure for 24 hr, the transcript expression level of *COX2* (inflammation-associated gene) was significantly upregulated, whereas that of *NFκB* remained the same as in the control cells. Thus, by 24 hr, the promotion of apoptosis in α-mangostin-treated SKOV-3 cancer cells had not reduced the inflammatory response. However, the changes in gene expression should be observed after longer exposures to α-mangostin, since *NFκB* plays a role in activating many inflammatory factors, such as TNF-α, interleukin (IL)-6, IL-8, matrix metalloproteinase, COX2, and nitric oxide synthase (39). It, therefore, remains plausible that α-mangostin may affect the expression of *NFκB* earlier (faster) than *COX2*.

For apigenin-treated SKOV-3 cancer cells, significantly increased caspase-9 activity was detected after 24 hr of exposure, which is the same timing as the onset of early apoptosis. Hence, the death of apigenin-treated SKOV-3 cells was likely to have been induced by the intrinsic pathway.

The expression of *BCL2* (an anti-apoptotic gene) transcripts, but not those of *CTNNB1* (a proto-oncogene), was significantly upregulated by apigenin, implying that other biomolecules or pathways are involved in this apoptotic process. This notion is potentially supported by Otake *et al*. (40), who reported that the overexpression of *BCL2* in lymphocytes alone did not cause cancer, whereas the simultaneous overexpression of *BCL2* and *MYC* (a proto-oncogene) could induce aggressive B-cell malignancies, including lymphoma. However, berbamine, isolated from the *Berberis amurensis* plant, could suppress the growth and invasion of the human ovarian cancer cell lines SKOV-3 and ES2 by inducing apoptosis via the increased activity of caspase-3 and -9 and the decreased expression of *BCL2* (3).

In the future, in order to enhance the efficacy of α-mangostin and apigenin as chemotherapeutic agents for ovarian cancer, other application approaches could be applied, such as with fatty acid-conjugated compounds (41), or the synergistic inhibition induced by co-administration with other promising compounds (42). Moreover, the toxicity of these compounds in an *in vivo* model system, such as the rat, should be determined (43,44).

ACKNOWLEDGMENTS

This work was financially supported by Chulalongkorn University, the Doctoral Degree Chulalongkorn University 100th Year Birthday Anniversary, the 90th Anniversary of Chulalongkorn University Fund (Ratchadaphiseksomphot Endowment Fund), Sci-Super IV_61_003, and the Overseas Research Experience Scholarship for Graduate Student.

CONFLICT OF INTEREST

The authors declare that there is no conflict of interest regarding the publication of this paper.

Received July 16, 2018; Revised September 7, 2018; Accepted October 4, 2018

REFERENCES

1. Reid, B.M., Permuth, J.B. and Sellers, T.A. (2017) Epidemiology of ovarian cancer: a review. *Cancer Biol. Med*., **14**, 9-32.
2. Li, J.X., Bi, Y.P., Wang, J., Yang, X., Tian, Y.F. and Sun, Z.F. (2018) JTC-801 inhibits the proliferation and metastasis of ovarian cancer cell SKOV3 through inhibition of the PI3K - AKT signaling pathway. *Pharmazie*, **73**, 283-287.
3. Zhang, H., Jiao, Y., Shi, C., Song, X., Chang, Y., Ren, Y. and Shi, X. (2018) Berbamine suppresses cell proliferation and promotes apoptosis in ovarian cancer partially via the inhibition of Wnt/β-catenin signaling. *Acta Biochim. Biophys. Sin. (Shanghai)*, **50**, 532-539.
4. Liotta, L.A., Steeg, P.S. and Stetler-Stevenson, W.G. (1991)

Cancer metastasis and angiogenesis: animbalance of positive and negative regulation. *Cell*, **64**, 327-336.
5. Luvero, D., Plotti, F., Lopez, S., Scaletta, G., Capriglione, S., Montera, R., Antonelli, G., Ciuffreda, S., Carassiti, R., Oliveti, A. and Angioli, R. (2017) Antiangiogenics and immunotherapies in cervical cancer: an update and future's view. *Med. Oncol.*, **34**, 115.
6. Ayla, Ş., Bilir, A., Ertürkoğlu, Ş., Tanrıverdi, G., Soner, B.C., Sofuoğlu, K., Ghisolfi, L. and Öktem, G. (2018) Effects of different drug treatments on the proliferation of human ovarian carcinoma cell line MDAH-774. *Turk. J. Med. Sci*., **48**, 441-448.
7. Rahman, N., Jeon, M., Song, H.Y. and Kim, Y.S. (2016) Cryptotanshinone, a compound of *Salvia miltiorrhiza* inhibits pre-adipocytes differentiation by regulation of adipogenesis-related genes expression via STAT3 signaling. *Phytomedicine*, **23**, 58-67.
8. Zhang, Y., Chen, S., Wei, C., Rankin, G.O., Rojanasakul, Y., Ren, N., Ye, X. and Chen, Y.C. (2018) Dietary Compound Proanthocyanidins from Chinese bayberry (*Myrica rubra* Sieb. et Zucc.) leaves inhibit angiogenesis and regulate cell cycle of cisplatin-resistant ovarian cancer cells via targeting Akt pathway. *J. Funct. Foods*, **40**, 573-581.
9. Zhang, Q., Dong, J., Cui, J., Huang, G., Meng, Q. and Li, S. (2018) Cytotoxicity of synthesized 1,4-naphthoquinone oxime derivatives on selected human cancer cell lines. *Chem. Pharm. Bull*., **66**, 612-619.
10. Puglisi, M.P., Bradaric, M.J., Pontikis, J., Cabai, J., Weyna, T., Tednes, P., Schretzman, R., Rickert, K., Cao, Z. and Andrei, D. (2018) Novel primary amine diazeniumdiolates-Chemical and biological characterization. *Drug Dev. Res*., **79**, 136-143.
11. Tsai, S.Y., Chung, P.C., Owaga, E.E., Tsai, I.J., Wang, P.Y., Tsai, J.I., Yeh, T.S. and Hsieh, R.H. (2016) Alpha-mangostin from mangosteen (*Garcinia mangostana* Linn.) pericarp extract reduces high fat-diet induced hepatic steatosis in rats by regulating mitochondria function and apoptosis. *Nutr. Metab. (Lond.)*, **13**, 88.
12. Nugitrangson, P., Puthong, S., Iempridee, T., Pimtong, W., Pornpakakul, S. and Chanchao, C. (2016) *In vitro* and *in vivo* characterization of the anticancer activity of Thai stingless bee (*Tetragonula laeviceps*) cerumen. *Exp. Biol. Med*., **241**, 166-176.
13. Sándor, Z., Mottaghipisheh, J., Veres, K., Hohmann, J., Bencsik, T., Horváth, A., Kelemen, D., Papp, R., Barthó, L. and Csupor, D. (2018) Evidence supports tradition: the *in vitro* effects of Roman chamomile on smooth muscles. *Front. Pharmacol*., **9**, 323.
14. Chantarudee, A., Phuwapraisirisan, P., Kimura, K., Okuyama, M., Mori, H., Kimura, A. and Chanchao, C. (2012) Chemical constituents and free radical scavenging activity of corn pollen collected from Apis mellifera hives compared to floral corn pollen at Nan, Thailand. *BMC Complement. Altern. Med*., **12**, 45.
15. Sivaranjani, M., Srinivasan, R., Aravindraja, C., KaruthaPandian, S. and Veera Ravi, A. (2018) Inhibitory effect of α-mangostin on Acinetobacter baumannii biofilms - an *in vitro* study. *Biofouling*, **34**, 579-593.
16. Chen, G., Li, Y., Wang, W. and Deng, L. (2018) Bioactivity and pharmacological properties of α-mangostin from the mangosteen fruit: a review. *Expert Opin. Ther. Pat*., **28**, 415-427.
17. Kumar, K.S., Sabu, V., Sindhu, G., Rauf, A.A. and Helen, A. (2018) Isolation, identification and characterization of apigenin from Justicia gendarussa and its anti-inflammatory activity. *Int. Immunopharmacol*., **59**, 157-167.
18. Abu Bakar, F.I., Abu Bakar, M.F., Rahmat, A., Abdullah, N., Sabran, S.F. and Endrini, S. (2018) Anti-gout potential of Malaysian medicinal plants. *Front. Pharmacol*., **9**, 261.
19. El Habbash, A.I., Mohd Hashim, N., Ibrahim, M.Y., Yahayu, M., Omer, F.A.E., Abd Rahman, M., Nordin, N. and Lian, G.E.C. (2017) *In vitro* assessment of anti-proliferative effect induced by α-mangostin from Cratoxylum arborescens on HeLa cells. *PeerJ*, **5**, e3460.
20. Suh, Y.A., Jo, S.Y., Lee, H.Y. and Lee, C. (2015) Inhibition of IL-6/STAT3 axis and targeting Axl and Tyro3 receptor tyrosine kinases by apigenin circumvent taxol resistance in ovarian cancer cells. *Int. J. Oncol*., **46**, 1405-1411.
21. Tang, A.Q., Cao, X.C., Tian, L., He, L. and Liu, F.(2015) Apigenin inhibits the self-renewal capacity of human ovarian cancer SKOV3-derived sphere-forming cells. *Mol. Med. Rep*., **11**, 2221-2226.
22. Niu, W., Chen, F., Wang, J., Qian, J. and Yan, S. (2017) Antitumor effect of sikokianin C, a selective cystathionine β-synthase inhibitor, against human colon cancer *in vitro* and *in vivo*. *Medchemcomm*, **9**, 113-120.
23. Fang, A., Zhang, Q., Fan, H., Zhou, Y., Yao, Y., Zhang, Y. and Huang, X. (2017) Discovery of human lactate dehydrogenase A (LDHA) inhibitors as anticancer agents to inhibit the proliferation of MG-63 osteosarcoma cells. *MedChemComm*, **8**, 1720-1726.
24. Xu, X., Rawling, T., Roseblade, A., Bishop, R. and Ung, A.T. (2017) Antiproliferative activities of alkaloid-like compounds. *MedChemComm*, **8**, 2105-2114.
25. Koopman, G., Reutelingsperger, C.P., Kuijten, G.A., Keehnen, R.M., Pals, S.T. and van Oers, M.H. (1994) Annexin V for flow cytometric detection of phosphatidylserine expression on B cells undergoing apoptosis. *Blood*, **84**, 1415-1420.
26. Schutte, B., Nuydens, R., Geerts, H. and Ramaekers, F. (1998) Annexin V binding assay as a tool to measure apoptosis in differentiated neuronal cells. *J. Neurosci. Methods*, **86**, 63-69.
27. Easton, D.F., Bishop, D.T., Ford, D. and Crockford, G.P. (1993) Genetic linkage analysis in familial breast and ovarian cancer: results from 214 families. The Breast Cancer Linkage Consortium. *Am. J. Hum. Genet.*, **52**, 678-701.
28. Yin, L., Li, J., Wei, Y., Ma, D., Sun, Y. and Sun, Y. (2018) Primary ovarian small cell carcinoma of pulmonary type with coexisting endometrial carcinoma in a breast cancer patient receiving tamoxifen: A case report and literature review. *Medicine (Baltimore)*, **97**, e10900.
29. Zhang, L., Shin, V.Y., Chai, X., Zhang, A., Chan, T.L., Ma, E.S., Rebbeck, T.R., Chen, J. and Kwong, A. (2018) Breast and ovarian cancer penetrance of BRCA1/2 mutations among Hong Kong women. *Oncotarget*, **9**, 25025-25033.
30. Reuter, S., Gupta, S.C., Chaturvedi, M.M. and Aggarwal, B.B. (2010) Oxidative stress, inflammation, and cancer: how are they linked? *Free Radic. Biol. Med*., **49**, 1603-1616.

31. Weinberg, F. and Chandel, N.S. (2009) Reactive oxygen species-dependent signaling regulates cancer. *Cell. Mol. Life Sci*., **66**, 3663-3673.
32. Chan, D.W., Liu, V.W., Tsao, G.S., Yao, K.M., Furukawa, T., Chan, K.K. and Ngan, H.Y. (2008) Loss of MKP3 mediated by oxidative stress enhances tumorigenicity and chemoresistance of ovarian cancer cells. *Carcinogenesis*, **29**, 1742-1750.
33. Kang, K.A. and Hyun, J.W. (2017) Oxidative stress, Nrf2 and epigenetic modification contribute to anticancer drug resistance. *Toxicol. Res*., **33**, 1-5.
34. Yurdacan, B., Egeli, U., Eskiler, G.G., Eryilmaz, I.E., Cecener, G. and Tunca, B. (2018) The role of usnic acid-induced apoptosis and autophagy in hepatocellular carcinoma. *Hum. Exp. Toxicol*., doi:10.1177/0960327118792052 [Epub ahead of print].
35. Boehning, A.L., Essien, S.A., Underwood, E.L., Dash, P.K. and Boehning, D. (2018) Cell type-dependent effects of ellagic acid on cellular metabolism. *Biomed. Pharmacother*., **106**, 411-418.
36. Hu,Y., Li, X., An, Y., Duan, J. and Yang, X.D. (2018) Selection of a novel CD19 aptamer for targeted delivery of doxorubicin to lymphoma cells. *Oncotarget*, **9**, 26605-26615.
37. Hupe, M.C., Hoda, M.R., Zengerling, F., Perner, S., Merseburger, A.S. and Cronauer, M.V. (2018) The BET-inhibitor PFI-1 diminishes AR/AR-V7 signaling in prostate cancer cells. *World J. Urol*., doi:10.1007/s00345-018-2382-8 [Epub ahead of print].
38. Hanan, N.A., Chiu, H.I., Ramachandran, M.R., Tung, W.H., MohamadZain, N.N., Yahaya, N. and Lim, V. (2018) Cytotoxicity of plant-mediated synthesis of metallic nanoparticles: a systematic review. *Int. J. Mol. Sci*., **19**, E1725.
39. Vallée, A. and Lecarpentier, Y. (2018) Crosstalk between peroxisome proliferator-activated receptor gamma and the canonical wnt/β-catenin pathway in chronic inflammation and oxidative stress during carcinogenesis. *Front. Immunol*., **9**, 745.
40. Otake, Y., Soundararajan, S., Sengupta, T.K., Kio, E.A., Smith, J.C., Pineda-Roman, M., Stuart, R.K., Spicer, E.K. and Fernandes, D.J. (2007) Overexpression of nucleolin in chronic lymphocytic leukemia cells induces stabilization of *bcl2* mRNA. *Blood*, **109**, 3069-3075.
41. Shibata, M.A., Hamaoka, H., Morimoto, J., Kanayama, T., Maemura, K., Ito, Y., Iinuma, M. and Kondo, Y. (2018) Synthetic α-mangostin dilaurate strongly suppresses wide-spectrum organ metastasis in a mouse model of mammary cancer. *Cancer Sci*., **109**, 1660-1671.
42. Xia, Y. and Sun, J. (2018) Synergistic inhibition of cell proliferation by combined targeting with kinase inhibitors and dietary xanthone is a promising strategy for melanoma treatment. *Clin. Exp. Dermatol*., **43**, 149-157.
43. Nurul, S.A.S., Hazilawati, H., Mohd, R.S., Mohd, F.H.R., Noordin, M.M. and Norhaizan, M.E. (2018) Subacute oral toxicity assessment of ethanol extract of *Mariposa christiavespertilionis* leaves in male Sprague Dawley rats. *Toxicol. Res*., **34**, 85-95.
44. Lee, Y. (2017) Cancer chemopreventive potential of procyanidin. *Toxicol. Res*., **33**, 273-282.